

## Crystal structures of human HSP90 $\alpha$ -complexed with dihydroxyphenylpyrazoles

Andreas Kreusch, Shulin Han, Achim Brinker, Vicki Zhou, Ha-soon Choi, Yun He, Scott A. Lesley, Jeremy Caldwell and Xiang-ju Gu\*

*Genomics Institute of the Novartis Research Foundation (GNF), 10675 John Jay Hopkins Drive, San Diego, CA 92121, USA*

Received 7 October 2004; revised 22 December 2004; accepted 29 December 2004

Available online 22 January 2005

**Abstract**—A series of dihydroxyphenylpyrazole compounds were identified as a unique class of reversible Hsp90 inhibitors. The crystal structures for two of the identified compounds complexed with the N-terminal ATP binding domain of human Hsp90 $\alpha$  were determined. The dihydroxyphenyl ring of the compounds fits deeply into the adenine binding pocket with the C2 hydroxyl group forming a direct hydrogen bond with the side chain of Asp93. The pyrazole ring forms hydrogen bonds to the backbone carbonyl of Gly97, the hydroxyl group of Thr184 and to a water molecule, which is present in all of the published HSP90 structures. One of the identified compounds (G3130) demonstrated cellular activities (in Her-2 degradation and activation of Hsp70 promoter) consistent with the inhibition of cellular Hsp90 functions.

© 2005 Elsevier Ltd. All rights reserved.

Heat-shock protein 90 (Hsp90) is an ATP-dependent molecular chaperone required for the stability and function of a number of 'client' proteins, some of them, such as Akt, Her2, and HIF-1 $\alpha$ , play important roles in promoting cancer cells growth and/or survival.<sup>1–4</sup> Several Hsp90 inhibitors including the natural products geldanamycin, radicicol and their derivatives (e.g., 17-desmethoxy-17-*N,N*-dimethylaminoethylamino-geldanamycin (17-DMAG) and 17-allylamino-17-demethoxy-geldanamycin (17-AAG)), as well as purine-<sup>5</sup> pyrazole-<sup>6,7</sup> and imidazopyrazine-based<sup>8</sup> small molecule synthetic compounds have been identified. The crystal structures for geldanamycin, radicicol, and purine derivatives complexed with the N-terminal ATP-binding domain of Hsp90 have been reported revealing a critical Asp residue at the bottom of the pocket for ligand binding.<sup>9–14</sup> Treatment of tumor cells with Hsp90 inhibitors causes selective degradation of Hsp90 client proteins and cell growth arrest and/or apoptosis in a number of cancer cell lines. It has been reported that the binding affinities of 17-AAG and a purine derivative, PU24FCL are much higher for tumor-derived HSP90 than for HSP90

derived from normal cells. And this selective inhibition of tumor HSP90 by geldanamycin and PU24FCL has been proposed to be the underlying mechanism of tumor selectivity of these compounds.<sup>15,16</sup> Currently, 17AAG is being tested in clinical trials against various cancers. However, 17-AAG has very limited solubility and is very difficult to formulate. Moreover, the presence of the quinone moiety in 17-AAG may contribute to its toxicity for normal tissues.

In order to increase the diversity of potential HSP90 inhibitors, we have developed a high throughput TR-FRET-based assay and used this assay to screen a diverse library of 1 million compounds.<sup>17</sup> Identified hits were confirmed in a [<sup>3</sup>H]-AAG binding assay and further characterized by a surface plasmon resonance (SPR) assay.<sup>17</sup> Several Hsp90 inhibitor scaffolds were identified. One class of compounds, the dihydroxyphenylpyrazoles (Fig. 1), are very similar to the compounds recently reported.<sup>6,7</sup> In the SPR assay, these compounds show reversible binding to the N-terminal ATP-binding domain of Hsp90 $\alpha$  with dissociation constants in the high nanomolar range (680 nM for compound G3129, and 280 nM for compound G3130) (Fig. 2).

High resolution crystal structures of the human HSP90 $\alpha$  N-terminal domain (residues 9–236) in complex

**Keywords:** Hsp90; Pyrazole; Dihydroxyphenylpyrazole; Co-crystal; 3D-structure; Structure based drug design.

\* Corresponding author. Tel.: +1 858 812 1565; fax: +1 858 812 1597; e-mail: [xgu@gnf.org](mailto:xgu@gnf.org)

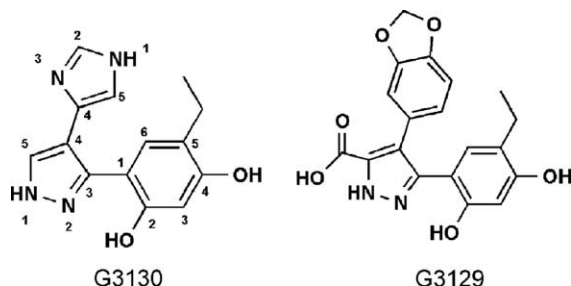


**Figure 1.** Structures of the identified dihydroxyphenylpyrazole compounds.

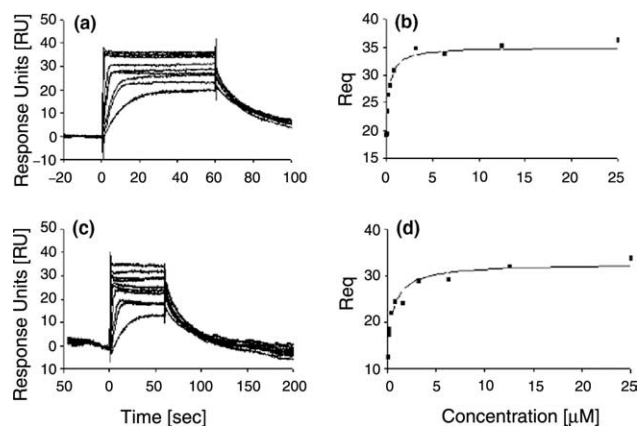


**Figure 2.** Reversible interaction of dihydroxyphenylpyrazole compounds with Hsp90 in the SPR assay. 5000RU of Hsp90N(M<sup>11</sup>C) was immobilized on a BIAcore biosensor chip and compounds were injected at increasing concentrations (49, 98, 195, 390, 780 nM, 1.56, 3.13, 6.25, 12.5, 25  $\mu$ M). Interaction kinetics was monitored and equilibrium binding signals ( $R_{eq}$ ) plotted against compound concentrations. Dissociation constants  $K_d$  were obtained by fitting a simple 1:1 binding model to the titration curves. (a) Kinetics of G3129-Hsp90 interaction. (b) Titration of G3129-Hsp90N interaction,  $K_d$  = 680 nM. (c) Kinetics of G3130-Hsp90 interaction. (d) Titration of G3130-Hsp90 interaction,  $K_d$  = 280 nM.

with two of the dihydroxyphenylpyrazole compounds (G3129 and G3130) were solved by molecular replacement using the co-crystal structure of HSP90 with 17-DMAG<sup>10</sup> as the initial model. All complexes described here showed excellent positive difference Fourier density for the compounds in the HSP90 binding pocket. In addition to the previously reported space groups  $P2_1$  and  $I222$  for co-crystal structures of the human HSP90 N-domain,<sup>9,10,13</sup> we observed a new crystal form,  $C222_1$ . The most significant conformational difference between various crystal forms concerns residues 108–114, the most flexible region in the N-terminal domain of HSP90. In the  $P2_1$  crystal form, this loop region adopts an ‘open’ ADP binding site conformation as opposed to the ‘closed’ conformation found in Apo HSP90 structures.<sup>9</sup> The  $C222_1$  form shows a slightly perturbed ‘open’ conformation, most likely due to crystal packing interactions (Fig. 3). After excluding the flexible loop region 106–130, a superposition of the  $C222_1$  form onto the  $P2_1$  form results in a root mean square deviation of only 0.4 Å for all remaining common C $\alpha$  atoms (184 atoms).

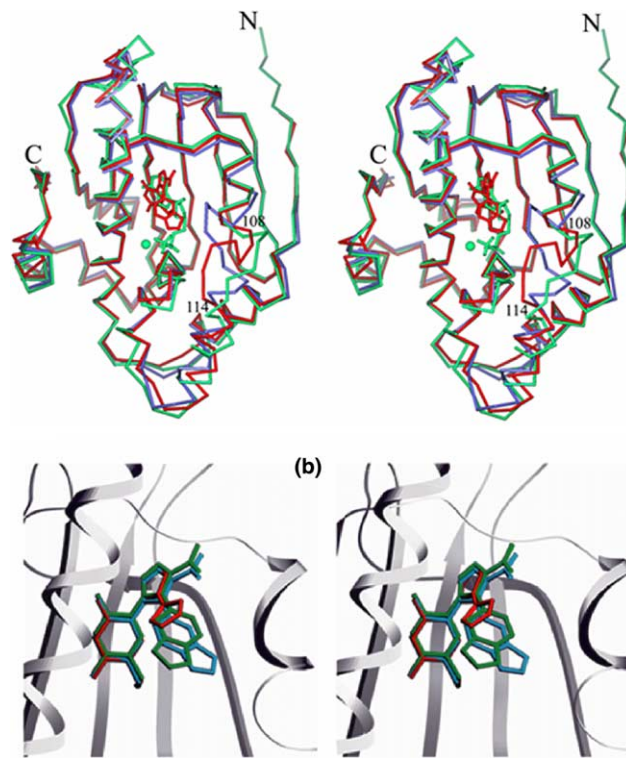


**Figure 3.** (a) Stereoview of the superimposed C $\alpha$  backbones from Apo-HSP90 (blue), ADP-HSP90 (green), and the  $C222_1$  crystal form of HSP90-G3129 (red). ADP is shown in green and the Mg<sup>2+</sup> ion is depicted as green sphere. Compound G3129 is shown in red and binds at the ADP-binding site. N- and C-termini are labeled. The loop region between residues 108 and 114 displays a high degree of flexibility, ranging from a ‘closed’ conformation in Apo-HSP90 to an ‘open’ conformation in the ADP-HSP90 and HSP90-G3129 co-crystal structures. (b) Stereoview of the superposition of the compound binding in all three co-crystal structures. The protein is depicted as a ribbon diagram (gray), compound G3129 in space group  $P2_1$  in green, compound G3129 in space group  $C222_1$  in blue, and compound G3130 in space group  $C222_1$  in red. Figures 3 and 5 have been generated with SETOR.<sup>19</sup>

Our compounds mimic the binding of ATP/ADP to HSP90 (Fig. 3) and maintain through their C2 hydroxyl a hydrogen bond to the side chain of Asp93, a residue, which has been previously identified to be critical for ATP binding<sup>11</sup> (Fig. 4). Additional interactions between the adenine ring of ATP and protein residues of the binding pocket are bridged by several water molecules.<sup>11</sup> Three of those water molecules are also present in our structures. Two of the three water molecules interact directly with the hydroxyl groups of our compounds. The C2 hydroxyl interacts through one of the conserved water molecules with the amide of Gly97. The C4 hydroxyl interacts via a network of two integral water molecules with the main chain carbonyls of Leu48, Ile91, and Thr184 as well as with the side chains from Ser52 and Asp93, respectively (Figs. 4 and 5). The dihydroxyphenyl ring of G3129/G3130 fits deep into the adenine binding pocket. The ethyl group of the dihydroxyphenyl ring protrudes into a hydrophobic pocket created by residues Phe138, Leu107, Val150, Met98, Val186, and Leu103 (Figs. 4 and 5). The size of the hydrophobic pocket is large enough to accommodate a bulkier

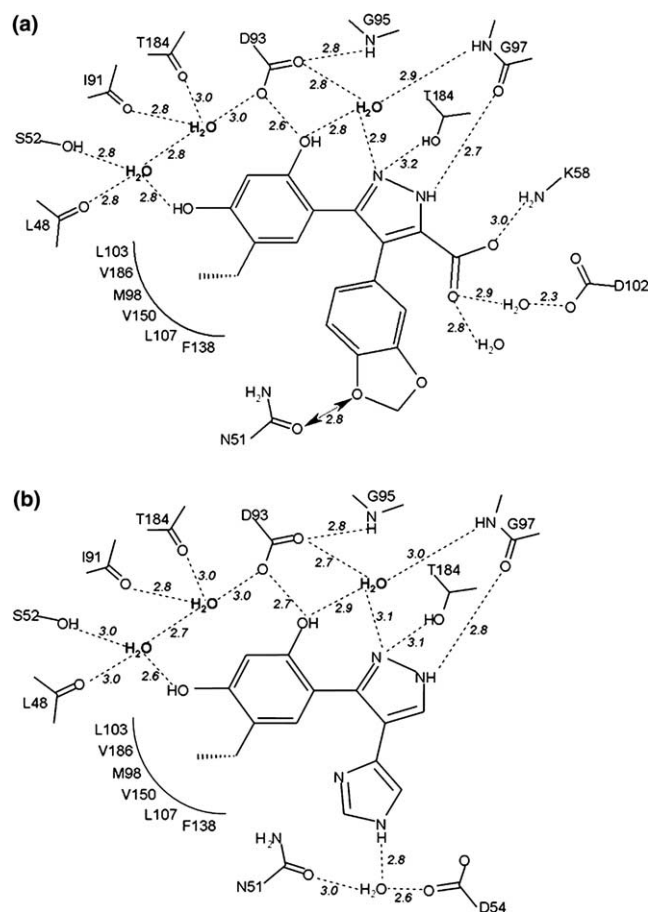


**Figure 4.** Schematic drawing of the interactions between the compounds and Hsp90. Integral water molecules conserved in Hsp90 structures are in bold. Hydrogen bonds are drawn as dotted lines with distances in Ångström. (a) Interactions of G3129 and Hsp90 in space group  $P2_1$ . The close proximity of the oxol oxygen to the side chain of Asn51 is depicted by an arrow. This particular interaction is absent in the  $C222_1$  crystal form due to a  $180^\circ$  flip of the benzodioxole ring. (b) Interactions of G3130 with Hsp90.

substitution at the C5 position of the dihydroxyphenyl ring (Fig. 5). This was recently confirmed by Dymock et al. where a phenyl ring of one of their purine-based

compounds can be accommodated by this lipophilic pocket.<sup>12</sup>

In our compounds, the pyrazole NH-1 forms a hydrogen bond to the backbone carbonyl of Gly97 while N-2 forms a hydrogen bond to the hydroxyl group of Thr184. Both pyrazole nitrogen atoms are also in close contact to one of the integral water molecules mentioned above (Figs. 4 and 5). This particular water molecule is in hydrogen-bonding distance to the carboxylate group of Asp93, the hydroxyl group of Thr184, and the backbone amide of Gly97 and is not only conserved in our crystal structures, but is also present in the apo-HSP90, the ADP-bound structures and in all reported inhibitor co-crystal structures.<sup>9–14</sup>

The carboxyl group at C5 of the pyrazole ring in G3129 forms a salt bridge to Lys58 as well as hydrogen bonds to two nearby water molecules. The imidazole ring in compound G3130 does not interact directly with HSP90, however, its imidazole NH-1 forms a polar interaction with a water molecule, which in turn forms hydrogen bonds to the side chains of Asn51 and Asp54, respectively (Fig. 5).

The benzodioxole ring in G3129 exists in two different conformations depending on the space groups we observed (Fig. 3). However, neither conformation results in direct interactions with the protein. In space group  $P2_1$ , a benzodioxole oxygen is only 2.8 Å away from Asn51-O<sub>6</sub> (Fig. 4). A flip of the side chain of Asn51 could lead to a favorable interaction between the amide and the benzodioxole moiety. In order to test this hypothesis, we flipped the side chain of Asn51, and after a least-squares refinement in combination with a B-factor refinement, it became clear that the resulting B-factor difference between the carbonyl and the amide of the side chain of Asn51 strongly supported the originally assigned conformation. It should be noted that the carbonyl oxygen of Asn51 is one of the ligands for the  $Mg^{++}$  ion in the ADP-bound HSP90 structure while the amide group forms a polar interaction with the  $\alpha$ -phosphate group of ADP and interacts via a water molecule with N7 of the adenine ring of ADP.<sup>11,14</sup>

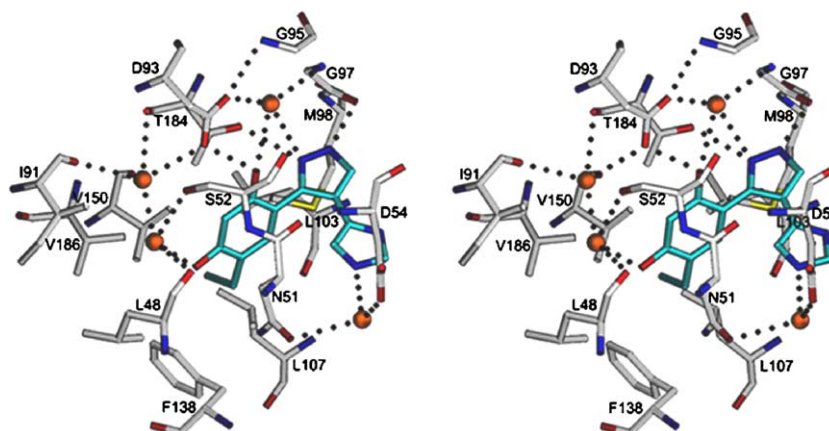


**Figure 5.** Stereoview of the interactions between HSP90 and compound G3130 (green). Water molecules are shown as orange spheres, hydrogen bond interactions are shown as dotted lines.



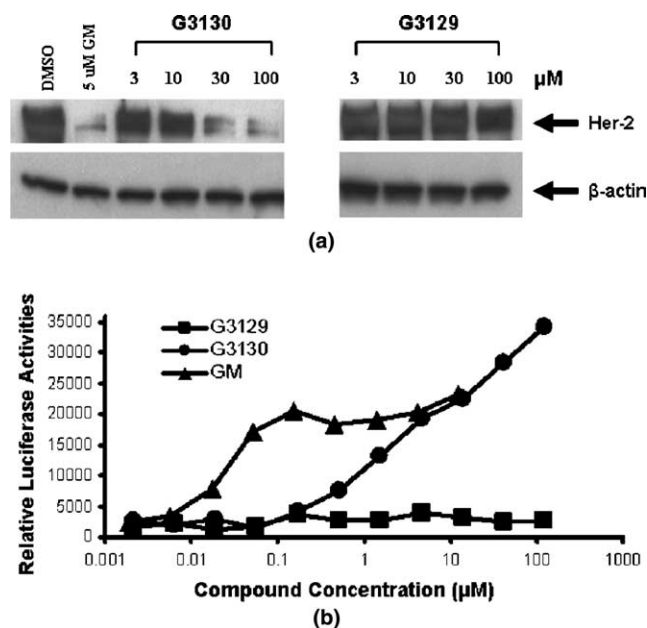


**Figure 6.** Cellular activities of the dihydroxyphenylpyrazole compounds. (a) Degradation of Her-2 induced by dihydroxyphenylpyrazoles in SKBR-3 cells. (b) Activation of the Hsp70 promoter-driven luciferase in 293T cells.

We expected that the presence of a salt bridge between Lys58 and the C5 carboxylate in G3129 should contribute to a stronger binding of G3129 over G3130, considering that all other interactions between HSP90 and the two compounds are essentially identical. However, the  $K_d$  value for G3130 is 0.28  $\mu$ M while G3129 has a  $K_d$  value of 0.68  $\mu$ M, indicating that the water mediated polar interaction between the imidazole NH-1 of G3130 and Asn51/Asp54 might be one of the important determinants for inhibition of HSP90 as has been observed for geldanamycin.<sup>18</sup>

To measure the activities of these compounds against Hsp90 in cells, we tested the effect of these compounds in causing Her-2 degradation and in inducing Hsp70 gene expression. Her-2 is one of the Hsp90 client proteins, which are most sensitive to the inhibition of Hsp90 function. All of the known Hsp90 inhibitors identified so far cause Her-2 degradation. Hsp70 induction is another hall mark of Hsp90 inhibition. As shown in Figure 6a, compound G3130 causes Her-2 degradation in SKBR-3 cells at 30  $\mu$ M. In the same experiment, geldanamycin cause Her-2 degradation at 5  $\mu$ M. Compound G3130 also causes the induction of Hsp70 promoter driven luciferase in 293T cells (Fig. 6b). In contrast, compound G3129 showed no significant cellular activity even at 100  $\mu$ M. The presence of a carboxylate group in compound G3129 may prevent the compounds from getting into the cells.

In conclusion, we have identified several dihydroxyphenylpyrazole compounds as reversible HSP90 inhibi-

tors. The crystal structures of these inhibitors complexed with HSP90 provide structural insights, which could be used in the design of more potent HSP90 inhibitors.

### Acknowledgements

We would like to thank Daniel McMullan and Heath Klock for protein expression and purification, Ariane Jansma for the determination of the compounds structure by NMR spectroscopy. We also appreciate the staff at the ALS for beamline assistance.

Crystallographic coordinates have been deposited with the Protein Data Bank: 1YC1 (G3129-C222<sub>1</sub>), 1YC3 (G3129-P2<sub>1</sub>), 1YC4 (G3130-C222<sub>1</sub>).

### References and notes

- Neckers, L.; Ivy, S. P. *Curr. Opin. Oncol.* **2003**, *15*, 419.
- Workman, P. *Curr. Cancer Drug Targets* **2003**, *3*, 297.
- Whitesell, L.; Bagatell, R.; Falsey, R. *Curr. Cancer Drug Targets* **2003**, *3*, 349.
- Solit, D. B.; Scher, H. I.; Rosen, N. *Sem. Oncol.* **2003**, *30*, 709.
- Chiosis, G.; Lucas, B.; Shtil, A.; Huez, H.; Rosen, N. *Bioorg. Med. Chem.* **2002**, *10*, 3555.
- Drysdale, M. J.; Dymock, B. W.; Barril-Alonso, X.; Workman, P.; Pearl, L. H.; Prodromou, C.; MacDonald, E. PCT Int. Appl. WO 2003055860, 2003.
- Beswick, M. C.; Brough, P. A.; Drysdale, M. J.; Dymock, B. W. PCT Int. Appl. WO 2004/050087, 2004.
- Currie, K. S.; DeSimone, R. W.; Pippin, D. A.; Darrow, J. W.; Mitchell, S. A. PCT Int. Appl. WO 2004/050087, 2004.
- Stebbins, C. E.; Russo, A. A.; Schneider, C.; Rosen, N.; Hartl, F. U.; Pavletich, N. P. *Cell* **1997**, *89*, 239.
- Jez, J. M.; Chen, J. C.-H.; Rastelli, G.; Stroud, R. M.; Santi, D. V. *Chem. Biol.* **2003**, *10*, 361.
- Prodromou, C.; Roe, S. M.; O'Brien, R.; Ladbury, J. E.; Piper, P. W.; Pearl, L. H. *Cell* **1997**, *90*, 65.
- Dymock, B.; Barril, X.; Beswick, M.; Collier, A.; Davies, N.; Drysdale, M.; Fink, A.; Fromont, C.; Hubbard, R. E.; Massey, A.; Surgenor, A.; Wright, L. *Bioorg. Med. Chem. Lett.* **2004**, *14*, 325.
- Wright, L.; Barril, X.; Dymock, B.; Sheridan, L.; Surgenor, A.; Beswick, M.; Drysdale, M.; Collier, A.; Massey, A.; Davies, N.; Fink, A.; Fromont, C.; Aherne, W.; Boxall, K.; Sharp, S.; Workman, P.; Hubbard, R. E. *Chem. Biol.* **2004**, *11*, 775.
- Roe, S. M.; Prodromou, C. P.; O'Brien, R.; Ladbury, J. E.; Piper, P. W.; Pearl, L. H. *J. Med. Chem.* **1999**, *42*, 260.
- Kamal, A.; Thao, L.; Sensintaffar, J.; Zhang, L.; Boehm, M. F.; Fritz, L. C.; Burrows, F. J. *Nature* **2003**, *425*, 407.
- Vilenchik, M.; Solit, D.; Basso, A.; Huez, H.; Lucas, B.; He, H.; Rosen, N.; Spampinato, C.; Modrich, P.; Chiosis, G. *Chem. Biol.* **2004**, *11*, 787.
- Zhou, V.; Han, S.; Brinker, A.; Klock, H.; Caldwell, J.; Gu, X. *Anal. Biochem.* **2004**, *331*, 349.
- Clevenger, R. C.; Blagg, S. J. *Org. Lett.* **2004**, *6*, 4459.
- Evans, S. V.; SETOR J. *Mol. Graphics* **1993**, *11*, 134.